Monte Carlo study of gating and selection in potassium channels

Daniele Andreucci,[*] Dario Bellaveglia,[†] Emilio N. M. Cirillo,[‡] and Silvia Marconi[§]
Dipartimento di Scienze di Base e Applicate per l'Ingegneria, Sapienza Università di Roma, via A. Scarpa 16, I-00161 Roma, Italy
(Received 6 May 2011; revised manuscript received 17 July 2011; published 19 August 2011)

The study of selection and gating in potassium channels is a very important issue in modern biology. Indeed, such structures are known in essentially all types of cells in all organisms where they play many important functional roles. The mechanism of gating and selection of ionic species is not clearly understood. In this paper we study a model in which gating is obtained via an affinity-switching selectivity filter. We discuss the dependence of selectivity and efficiency on the cytosolic ionic concentration and on the typical pore open state duration. We demonstrate that a simple modification in the way in which the selectivity filter is modeled yields larger channel efficiency.

DOI: 10.1103/PhysRevE.84.021920 PACS number(s): 87.10.−e, 87.16.−b, 66.10.−x

I. INTRODUCTION

Potassium currents across nerve membranes have been studied for a long time (see, for instance, [1–3] and the reviews [4–8]). It is now known that ionic channels selecting potassium currents are present in almost all types of cells in all organisms and that they play many important and different functional roles.

An important improvement in experiments was the appearance of the *patch clamp* technique (see for instance [9]) which permitted the measurement of the ionic current flowing through a single channel on the cell membrane. Different types of measurements (see for instance [10,11]) provide a very detailed description of the behavior of potassium channels. Less is known on their structure [6]; some things have been inferred starting from functional behavior and some have been deduced via direct inspection.

Despite the large variety of ionic channel types, they all form selective pores in the cell membrane which open and close stochastically and, when in the open state, allow permeation of a selected ionic species (potassium in K^+ channels). Gating (i.e., their ability to open and close) and selectivity (i.e., their ability to allow the flux of a particular ionic species in the cytoplasm) are not yet completely understood. The way in which gating and selection are achieved can be different from channel to channel [6].

On theoretical grounds this problem has been approached with a large variety of methods. Molecular dynamics studies [12] give a very detailed description of the phenomenon and their results can also be compared with structural experimental information, but they are usually not able to provide macroscopic current estimates due to the too small involved time scale. A different approach is that of kinetic models [13–17] which give very useful information since electrophysiological experiments are performed over time scales much longer than the atomic one. The drawback is represented by the extreme simplifications on the structure of the channel.

Models such as the ones in [14–16] describe to some extent the dynamics of ion permeation through the selectivity filter (see also [17]). In this paper, following [18], we introduce a model where the channel is lumped to a two state stochastic point system. A remarkable feature of our model is the interaction between the dynamics of the ions inside the cell and that of the selectivity filter itself.

In Ref. [18] a very simplified model for the pore behavior has been proposed. The main idea is that the pore can be in two states, *high* and *low* affinity. In the former, potassium ions can bind to molecules inside the pore, while smaller sodium ions cannot. In the latter, on the other hand, no ion can bind to the pore. We then have that when the pore is in the low-affinity state, the two ionic species permeate in the same way. On the contrary, when the pore is the high-affinity state, sodium particles are reflected by the pore, while potassium ions bind to it and, eventually, when the pore comes back to the low-affinity state, dissociate and possibly exit the cell. This selectivity mechanism controls the potassium flux through the cell membrane and, hence, yields gating. In [18] it was proven that it is possible to obtain gating via selection, but it was also noted that a pronounced reduction in the potassium flux is observed when the fraction of time the pore spends in the high-affinity state is large; indeed in this case for long periods of time no permeation is allowed.

For instance, the Kcv from chlorella virus PBCV-1 [10], which have no long cytosolic regions, are able to close and open in response to membrane voltage. For this kind of channel it is attractive to think that gating is indeed realized via selection [18]; in other words, researchers were led to suppose that different current levels are indeed obtained through the selection mechanism.

The basic motivation of this paper is to study the way in which the ion dynamics in cytosol affects the pore behavior and explore the possibility of reducing the potassium flux loss due to selection. In our model we assume that the ionic species diffuse in the cytosol through independent random walks on a two-dimensional lattice and, for the potassium and sodium flux ratio, we find results comparable to those in [18], where the motion of ions in cytosol was assumed to be uniform (constant velocity). As already noted in [18], good selection is obtained when the time fraction spent in the high-affinity state is chosen long enough. In this case, the

[*]daniele.andreucci@sbai.uniroma1.it
[†]dario.bellaveglia@sbai.uniroma1.it
[‡]emilio.cirillo@uniroma1.it
[§]silvia.marconi@sbai.uniroma1.it

potassium flux through the channel is remarkably reduced. Our results suggest that by modeling the cytosolic dynamics as a diffusive rather than uniform motion, the potassium flux loss is less important. Moreover, we prove that it is possible to compensate for this effect by just allowing the pore to stuff more than one particle at a time. For realistic concentrations of potassium inside the cell, it is seen that allowing three (in rare occurrences four) potassium ions to be packed in the pore, when it is in the high-affinity state, is enough to compensate for the potassium flux reduction due to the selectivity filter. This hypothesis is compatible with what is known about the structure of potassium channels [12,14].

We also perform an extensive study of the dependence of fluxes on the two main physiological parameters, namely, the fraction of time the pore spends in the high-affinity state and the concentration of the ions in the cell. As it is easy to guess, the sodium flux is directly proportional to the ionic density in the cell. For potassium ions, on the other hand, this linear behavior is found only for small values of the time fraction spent in the high-affinity state (in this case the two ionic species behave similarly), while for large values of such a time fraction a sublinear behavior is found. We studied the behavior of fluxes as a function of the time fraction spent in the low-affinity state at fixed ionic concentration; we found a sublinear increasing behavior for both sodium and potassium.

Since the pore is modeled in a very simple way (a two state random variable independent by the random walk dynamics inside the cell), it is possible to analytically study the model. We perform an approximate study in the two-dimensional case and we are able to explain the results found via the Monte Carlo simulation. The most interesting effect that is pointed out by this analysis is that the sublinear behavior discussed above is due to a sort of depletion of the region close to the pore, which is observed when the typical time spent by the pore in the low-affinity state is large. The one-dimensional model has been studied to some extent exactly in order to support our approximate two-dimensional analysis and to test the reliability of our Monte Carlo computation.

The paper is organized as follows. In Sec. II we introduce the model, describe the quantities that are measured with the Monte Carlo procedure, and give their physical interpretation. Sections III–V are devoted to the discussion of our numerical results: we first focus on the possibility of realizing gating via selection and on the way in which the potassium flux loss can be reduced; then we discuss the dependence of the fluxes on the physiological parameters of the model. In Sec. VI we give an approximate analytical study of the two-dimensional model and in Sec. VII we summarize our conclusions. Appendices are devoted to the detailed algorithmic definition of the model and to the exact one-dimensional study.

II. THE MODEL

The model that we study in this paper is inspired by the two-dimensional one proposed in [18]. We now give a quick glance to the model and postpone the precise description of the algorithm to Appendix A. The cytosolic region of the cell is modeled via a finite two-dimensional square lattice Λ with L^2 sites, where L is an odd integer [see Fig. 1 (left)]. We consider a two-dimensional model for simplicity, but as it will be discussed in the sequel, the model is able to capture the main features of the real behavior. Two ionic species perform independent symmetric random walks on the lattice with reflectivity conditions on the boundary $\partial\Lambda$ of the volume Λ. One site of the boundary is special and it is called *pore*; its behavior, that will be described below, makes the potassium walkers not independent. The number of potassium and sodium walkers are, respectively, denoted by N_{K} and N_{Na}. The fact that the walkers are independent on Λ means that the position of a particle does not affect the motion of the others, in particular, no constraint to the number of particles on each site is prescribed.

The pore is modeled by the site in the middle of one of the four sides of the boundary $\partial\Lambda$. Two states are allowed for the pore: *high-affinity* and *low-affinity*. The pore switches between the two states randomly; the probability that the pore is in the low-affinity state is denoted by p. The behavior of the particles on the site neighboring the pore depends on the state of the pore itself as it is precisely stated in Fig. 1. The idea is the following: if the pore site is in the low-affinity state, both potassium and sodium ions can enter it; when they enter the pore they immediately dissociate so that, with probability $1/2$, they reenter Λ and with the same probability exit the system. If the pore is in the high-affinity state, sodium ions are reflected by the pore site and potassium ions are reflected by the pore if it is occupied, while they can enter it if it is free. In this last case the ion does not dissociate immediately, but it remains bounded to the pore until its state is changed to the low-affinity one. As noted above, due to the pore rule, the sodium walkers are independent while the potassium ones are not.

Whenever an ion exits the system a particle of the same species is put at random with uniform probability $1/L^2$ on one of the L^2 sites in Λ so that the number of sodium and potassium ions in the system remains constant.

The model described above is implemented with the Monte Carlo algorithm which will be described in detail in Appendix A. An *iteration* or *sweep* of the Monte Carlo is the collection of the steps that are performed at each time t. The number of iterations that are performed in a simulation is $t_{\max}$.

A. Measured quantities and goal

The particles that exit the system model the outgoing ionic flux. This is precisely what we want to measure. For a single numerical experiment we let $M_{\mathrm{Na}}(t)$ $[M_{\mathrm{K}}(t)]$ be the number of sodium [potassium] particles which exited the system in the time interval $[0,t]$. Moreover, we let the sodium [potassium] *flux* $f_{\mathrm{Na}}(t)$ $[f_{\mathrm{K}}(t)]$ at time t be $M_{\mathrm{Na}}(t)/t$ $[M_{\mathrm{K}}(t)/t]$. Since we defined the Monte Carlo algorithm in such a way that the number of sodium and potassium ions keep constant in the volume Λ, both $f_{\mathrm{Na}}(t)$ and $f_{\mathrm{K}}(t)$ approach a constant value for $t \to \infty$. To estimate these limiting values, which are denoted by $\bar{f}_{\mathrm{Na}}$ and $\bar{f}_{\mathrm{K}}$, we perform different numerical experiments with number of iterations $t_{\max}$ sufficiently large, we then average the experimental measures $f_{\mathrm{Na}}(t_{\max})$ and $f_{\mathrm{K}}(t_{\max})$ and compute the associated statistical errors.

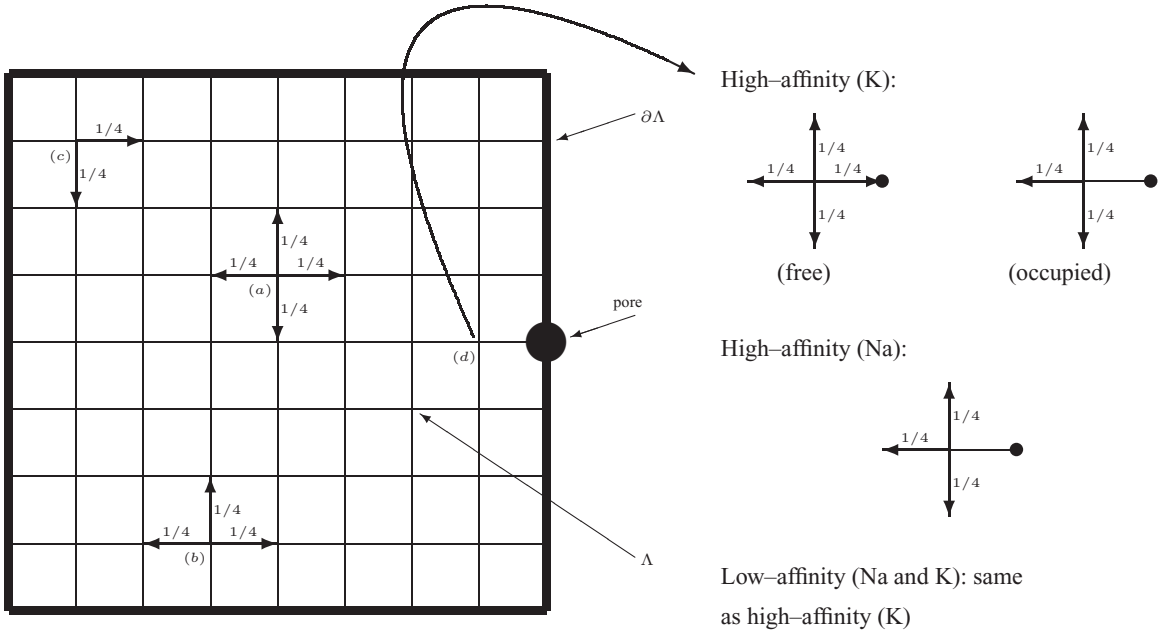

FIG. 1. On the left: thin line intersections represent the lattice sites; intersections between thin and thick lines represent the boundary sites. The pore is in the middle of the right-hand boundary side. (a) Rules for a particle in the bulk: the particle jumps with uniform probability 1/4 to one of the four nearest neighboring sites. (b) Rules for a particle close to the boundary: the particle jumps with uniform probability 1/4 to one of the three nearest neighboring sites in the lattice; with probability 1/4 the particle does not leave the site. (c) Rules for a particle in the corner: the particle jumps with uniform probability 1/4 to one of the two nearest neighboring sites in the lattice; with probability 1/2 the particle does not leave the site. (d) The rules for a particle in the site neighboring the pore depend on the state of the pore and are explained in the picture on the right. Pore in the high-affinity state (potassium): when the pore is free the particle jumps with uniform probability 1/4 to one of the four nearest neighboring sites (pore included); when the pore is occupied the particle jumps with uniform probability 1/4 to one of the three nearest neighboring sites in the lattice (it cannot enter the pore); and with probability 1/4 the particle does not leave the site. Pore in the high-affinity state (sodium): the particle jumps with uniform probability 1/4 to one of the three nearest neighboring sites in the lattice (it cannot enter the pore) and with probability 1/4 the particle does not leave the site. Pore in the low-affinity state: same rule as that for the potassium particle faced to the pore in the high-affinity state; it is worth remarking that the pore in the low-affinity state will never be occupied (see the description of the algorithm in the text).

Our aim is to measure $\bar{f}_{\mathrm{Na}}$ and $\bar{f}_{\mathrm{K}}$ and to prove that the model provides selection in an efficient way. The two ionic species interact in the same way with the pore in the low-affinity state (see the rules in Fig. 1); hence, when p is close to one, no difference should be observed in the potassium and sodium fluxes. A different behavior should be observed at smaller p, indeed when the pore is in the high-affinity state the sodium flux is blocked while some residual potassium flux should be recorded.

We shall then compute the ratio $\bar{f}_{\mathrm{K}}/\bar{f}_{\mathrm{Na}}$ and prove that it becomes large for small p. Moreover, we shall discuss if this selection mechanism is efficient, namely, we shall see that selection is provided with a potassium flux comparable with the flux measured when the pore is constantly in the low-affinity state. In particular, in the sequel we shall discuss a slightly different model which will provide selection without flux reduction.

B. Choice of the parameters

We first describe how the physiological parameters of the model have been chosen. We have considered different values of the number of potassium (N_{K}) and sodium (N_{Na}) particles. Although cytosol is typically much richer in potassium than in sodium, in order to check the efficiency of the selectivity filter, we have always taken $N_{\mathrm{Na}} = N_{\mathrm{K}}$. In all the simulations discussed in this section we have chosen $L = 101$, while we considered the cases

$$N_{\mathrm{Na}} = N_{\mathrm{K}} = 100,\ 1000,\ 3000,\ 5000,\ 10\,000$$

and

$$p = 0.001,\ 0.003,\ 0.005,\ 0.007,\ 0.01,\ 0.03,\ 0.05,\ 0.07,\ 0.1,\ 0.3,\ 0.5,\ 0.7,\ 1.$$

Note that the total time fraction the pore spends in the low-affinity state is essentially equal to $t_{\max} p$.

It is worth noting that, provided $L = 101$, the most physiologically reasonable choice for the number of potassium ions among those listed above seems to be $N_{\mathrm{K}} = 100$. This is supported by the following very rough computation. The concentration of potassium ions in cytosol is approximatively equal to $c = 150$ mM (millimolar), that is c mole per cubic meter. The radius of the potassium ion is $r = 1.52 \times 10^{-10}$ m; assuming that each site of the lattice can accommodate at most n ions, we can ascribe the volume $n(2r)^3$ to each site of the lattice. The number of potassium ions that must be put on the lattice is then

$$\text{number of potassium ions} = cL^2 n(2r)^3 n_{\mathrm{A}} = 25.88n$$

where $n_A = 6.02 \times 10^{23}$ is the Avogadro number, that is, the number of ions in a mole. Assuming that reasonable values of n ranges between 1 and 10, we have that realistic values of the number of potassium ions on the lattices ranges from 25 to 250.

The sole Monte Carlo parameter to be fixed is the number of sweeps t_{max}. As explained above, it must be taken large enough in order to get a good estimate of the outgoing fluxes. In all the cases that we considered it was sufficient to take $t_{max} = 10^7$.

III. GATING AND SELECTION

As it has already been stated, our first purpose is checking the behavior of the ratio $\bar{f}_K/\bar{f}_{Na}$ as a function of the probability p. Results are shown in Fig. 2: from the bottom to the top the ratio $\bar{f}_K/\bar{f}_{Na}$ for $N_{Na} = N_K = 10\,000$, 5000, 3000, 1000, 100 has been plotted as a function of p. We have that the ratio between the potassium and the sodium outgoing fluxes increases when the probability for the pore to be in the low-affinity state is decreased. This is precisely the result in [18]; in particular for $N_{Na} = N_K = 100$ our data are not only qualitatively but also quantitatively close to those in [18], although a different ion dynamics in the cytoplasm has been considered. As noted in [18] it is then possible to imagine a potassium channel in which gating is realized via the selectivity filter.

The log-log plots in Fig. 2 shows a straight line behavior for large p, say $p \geqslant 0.08$. Note that the threshold where the linear behavior starts is smaller for smaller values of the ionic density in cytosol. This means that in this regime, say $p \geqslant 0.08$, the ratio $\bar{f}_K/\bar{f}_{Na}$ can be well approximated by a power law

$$\frac{\bar{f}_K}{\bar{f}_{Na}} = a_1(p)^{-b_1}. \tag{1}$$

The coefficient a_1 and b_1 can be computed by fitting the data plotted in Fig. 2; we obtain $a_1 = 0.863$, 0.904, 0.974, 1.014, 1.072 and $b_1 = 0.860$, 0.798, 0.694, 0.616, 0.480, respectively, for $N_K = N_{Na} = 100$, 1000, 3000, 5000, 10 000.

It is worth noting that, if the density of ions in the cytosolic region is not too high, good selection ratios are reached at not too small p; this is good news, since too low values of p would imply very small ionic currents. In particular, good results are found for the physiologically reasonable parameters $N_{Na} = N_K = 100$. When the number of particles in the system is raised, the selection effects are widely reduced. This is quite intuitive, indeed, when the density is large, the average number of particles trying to enter the pore is large as well; in other words, the time between two consecutive attempts to enter the pore is small. If the typical duration of the intervals in which the pore stays in the high-affinity state is larger than this "knocking" time, a lot of attempts to enter the pore will abort since the filter is occupied by another particle. It is then clear that the selection mechanisms does not work in the optimal regime. In the sequel we shall propose a modified version of the model which will take care of this problem.

We have seen that the algorithm provides good selection for small enough p; at physiological concentrations, in order to get a ratio $\bar{f}_K/\bar{f}_{Na}$ larger than 100, the low-affinity state probability p must be chosen smaller than 0.01. In this regime we expect a potassium flux reduction with respect to the case $p = 1$. We estimate this loss by plotting in Fig. 3 the normalized potassium and sodium fluxes, namely, the ratio between fluxes at any p with the corresponding fluxes at $p = 1$. We first note that the flux reduction is more effective for the sodium ions rather than for the potassium ones; this is obvious since the selectivity filter favors potassium particles. Moreover, in the case of sodium particles, the reduction does not depend on the number of particles on the lattice and this is due to the fact that all the sodium related measured quantities are directly proportional to the sodium density in cytosol.

Potassium flux, on the other hand, experiences a remarkable loss at small low-affinity state probability p. This reduction gets more and more important as the density is increased. At physiological potassium density the flux reduction is about the 40% at very small low-affinity state probability. With respect to this point, it seems that our algorithm is more efficient than the one proposed in [18], indeed, in that paper, with a similar selection ability, larger potassium flux losses were found. In other words, the importance of potassium flux loss depends on how the cytosol dynamics is modeled, indeed in our model

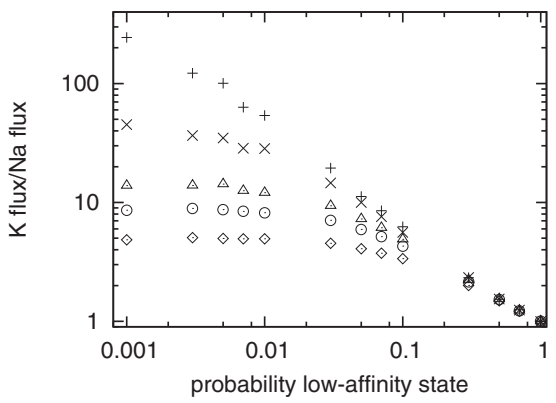

FIG. 2. Log-log plot of the ratio $\bar{f}_K/\bar{f}_{Na}$ as a function of the probability p. Data refers to the cases $N_{Na} = N_K = 10\,000(\diamond)$, $5000(\bigcirc)$, $3000(\triangle)$, $1000(\times)$, $100(+)$.

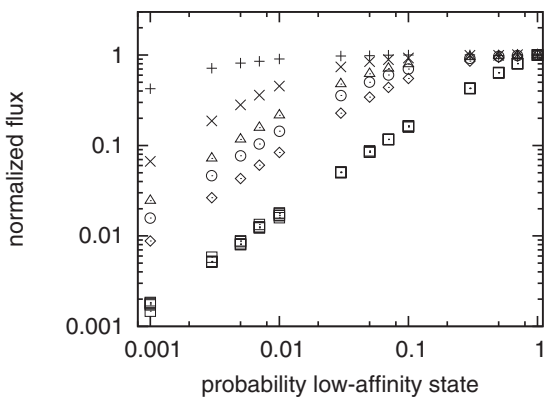

FIG. 3. Log-log plot of the normalized fluxes as functions of the low-affinity state probability p. For the potassium the data in the picture refers to the cases $N_K = 10\,000(\diamond)$, $5000(\bigcirc)$, $3000(\triangle)$, $1000(\times)$, $100(+)$; for the sodium we used the symbol $\square$ for the five cases $N_{Na} = 10\,000$, 5000, 3000, 1000, 100.

ions move inside the cell according to a symmetric random walk, while in [18] they perform a uniform motion until the boundary is reached. In the next section we propose a modified version of the model aiming to reduce potassium losses.

IV. IMPROVING EFFICIENCY

As it has been discussed above, the model which has been proposed before is able to describe the gating attitude of a potassium channel via a suitable selectivity filter.

The main problem with this approach is that the presence of the filter reduces the amount of the permeating potassium ions. To be more precise, in order to obtain a remarkable selection one has to assume that the time fraction in which the pore is in the low-affinity state is very small. From the data in Fig. 2 it follows that, at physiological concentrations, in order to get the ratio $\bar{f}_K/\bar{f}_{Na}$ larger or equal to 100 one has to assume $p \leqslant 0.1$. As shown in Fig. 3, at these values of the low-affinity state probability an important reduction of the potassium flux is observed.

This phenomenon has a simple explanation: at small p many attempts performed by K^+ ions to exit the cell abort since it often happens that the pore is in the high-affinity state and occupied by another potassium particle. This problem can be bypassed by assuming that more than one ion at a time can be accommodated in the pore. We test this idea in the simplest possible way without modeling the pore structure or any possible interaction between ions in the pore as it has been done in [18] (this is obviously a very interesting question deserving future investigation). We simply assume that there is no upper bound to the number of ions that can be accommodated in the pore (see below). In other words, when the filter is in the high-affinity state, a potassium particle can enter it even if the pore is currently occupied by one or more potassium ions.

This modified version of our model will assure no potassium flux reduction since all the potassium ions trying to enter the pore in the high-affinity state will be accepted and then will be released when the state of the filter switches to the low-affinity one.

This model will not be physiologically reasonable if the typical number of potassium ions stuffed inside the pore is large. From what it is known on the structure of ionic channels (see, for instance, [12,19,20]), a potassium channel is about 12 Å long and 2.5 Å in diameter. This means, recalling that the radius of a potassium ion is approximatively 1.5 Å, that at most four or five potassium particles can coexist inside the pore. We stress that in this simple model we do not take into account any interaction, for instance electrostatic repulsion, between ions in the pore. As we shall see, at physiological densities, that is, $N_{Na} = N_K = 100$ and for $p \geqslant 0.01$, the average number of potassium ions in the pore will be very low and at most four particles (in very rare cases) will be simultaneously accommodated inside the pore. We shall then conclude that in this regime our simple model is reasonable on physiological grounds.

The results are shown in Figs. 4 and 5. By comparing Figs. 4 and 2, it is clear that the selectivity attitude of the new model does not depend on the density of the ions in cytosol and that the modified model is more selective. Figure 5 is even more

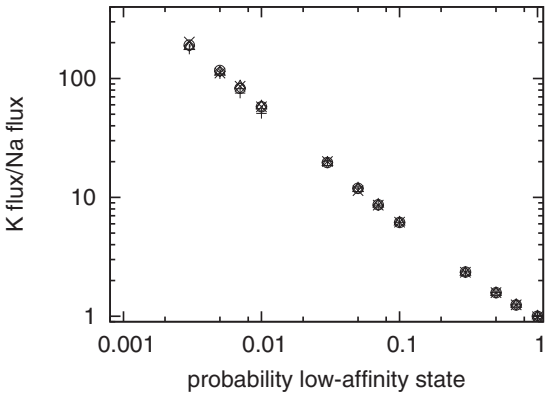

FIG. 4. Log-log plot of the ratio $\bar{f}_K/\bar{f}_{Na}$ as a function of the probability p for the modified model; this picture should be compared with Fig. 2. Data refers to the cases $N_{Na} = N_K = 10\,000$(⋄), 5000(◯), 3000(△), 1000(×), 100(+).

interesting, indeed it shows that the potassium flux does not depend on the low-affinity state probability. In other words, the model introduced in this section behaves precisely as we expected and, hence, it provides the solution to the potassium flux loss.

It is important now to discuss the physiological reasonableness of the model. In order to answer this question, which is very important in the present context, we have run a long simulation (about 3×10^7 sweeps) recording at each instant the number of potassium particles accommodated in the pore site. In the three cases $N_{Na} = N_K = 100, 1000, 5000$ [see Figs. 6(a)–6(c)] the number of simultaneously stuffed particles is, along the whole simulation, respectively, smaller than 4, 15, and 62.

It then follows that at physiological values of the cytosolic ion density, that is, for $N_{Na} = N_K = 100$ and for low-affinity state probability not too small ($p \geqslant 0.01$), the model is completely reasonable.

We can then conclude that a model of potassium channels is feasible in which the gating attitude is obtained via a selectivity

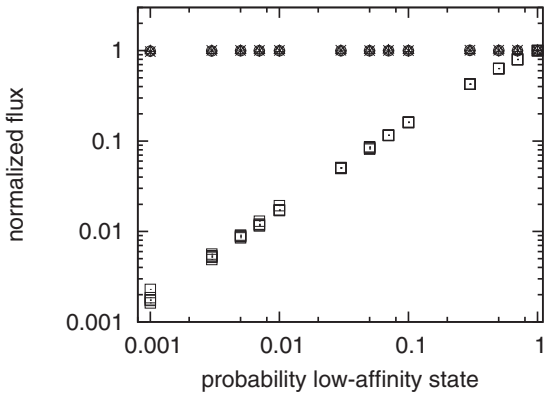

FIG. 5. Log-log plot of the normalized fluxes as functions of the low-affinity state probability p for the modified model; this picture should be compared with Fig. 3. For the potassium the data in the picture refers to the cases $N_K = 10\,000$(⋄), 5000(◯), 3000(△), 1000(×), 100(+); for the sodium we used the symbol □ for the five cases $N_{Na} = 10\,000, 5000, 3000, 1000, 100$.

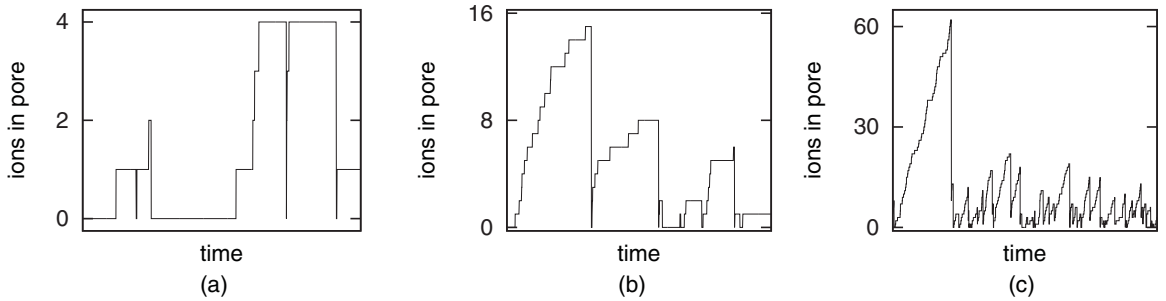

FIG. 6. Number of potassium ions accommodated inside the pore in an interval of time of few thousands sweeps out of 3×10^7 for the modified model. Parameters of the simulation: $p = 0.01$, (a) $N_{\mathrm{Na}} = N_{\mathrm{K}} = 100$, (b) $N_{\mathrm{Na}} = N_{\mathrm{K}} = 1000$, and (c) $N_{\mathrm{Na}} = N_{\mathrm{K}} = 5000$.

filter and such that the filter does not produce any potassium flux reduction.

V. DISCUSSION

We now discuss the behavior of the sodium and potassium flux in the basic model as a function of the two main physical parameters: the ionic cytosolic density and the time fraction in which the pore is in the low-affinity state (which, we recall, is essentially p). In this section we shall simply describe the numerical results; the next section will be devoted to their physical interpretation via a simple analytical model.

It is difficult to have an intuition on the potassium flux behavior, indeed the way in which the selectivity filter acts upon its current is not transparent at all. Since the filter acts simply as a gate on sodium, it is rather natural to expect that the sodium flux will be directly proportional to the sodium density on the lattice; on the other hand, the way in which it depends on the the low-affinity state probability, that is, on the time fraction the filter spends in the low-affinity state, cannot be easily guessed *a priori*.

We discuss first how the sodium flux depends on concentration in cytosol. In Fig. 7 we have plotted the sodium flux $\bar{f}_{\mathrm{Na}}$ as a function of the sodium density $\varrho_{\mathrm{Na}} = N_{\mathrm{Na}}/L^2$ on the lattice. Only the curves corresponding to the values

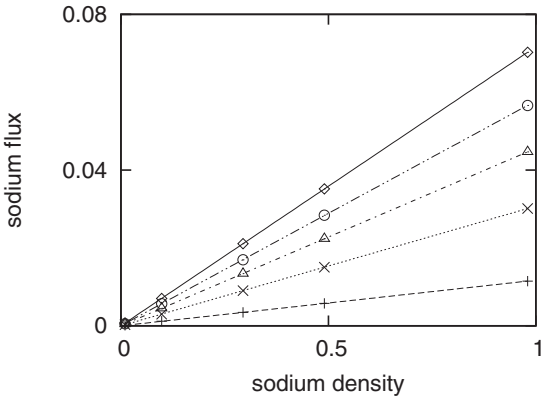

FIG. 7. Sodium flux $\bar{f}_{\mathrm{Na}}$ as a function of the sodium density ϱ_{Na}. Data in the picture refers to the cases $p = 1(\diamond)$, $0.7(\bigcirc)$, $0.5(\triangle)$, $0.3(\times)$, $0.1(+)$. The other values of p are not shown: the behavior is linear with smaller and smaller slope (see Table I). Note that the behavior in the picture is reasonable since the selectivity filter does not affect the sodium dynamics.

$p = 1, 0.7, 0.5, 0.3, 0.1$ are shown; other values of the low-affinity state probability yield similar results. As expected, the flux is directly proportional to the density with slope depending on the low-affinity state probability. We have fitted our data with the function

$$\bar{f}_{\mathrm{Na}} = a_2 + b_2 \varrho_{\mathrm{Na}} \tag{2}$$

and computed the parameters a_2 and b_2 for the different values of p; results are shown in Table I. It is very interesting to remark that the slope coefficient b_2 depends linearly on p in the interval [0,0.1]; for larger values of the low-affinity state probability the behavior departs from linearity. To illustrate this remark, in Fig. 8 we have plotted the coefficient b_2 as a function of p (we recall that the time fraction spent by the pore in the low-affinity state is, roughly speaking, equal to p). The picture shows that for small low-affinity state probabilities the slope b_2 is directly proportional to p, that is to the time fraction that the pore spends in the low-affinity state. This result is consistent with a theorem proven in [21] in a three-dimensional diffusion model.

The predictions of (2) with the coefficient a_2,b_2 chosen as in the caption of Fig. 8, that is,

$$\bar{f}_{\mathrm{Na}} = \varrho_{\mathrm{Na}} \frac{p}{a_3' + b_3' p}, \tag{3}$$

are compared with the experimental data in Fig. 9 and the matching is striking.

We now come to the results related to the potassium flux. Potassium flux as a function of potassium density in the lattice bulk $\varrho_{\mathrm{K}} = N_{\mathrm{K}}/L^2$ has been plotted in Fig. 10. In this case the behavior is approximatively linear for values of the low-affinity state probability p close to one. But at smaller values of p the graph remarkably departs from linearity. In other words, when

TABLE I. Values of the parameters a_2 and b_2 introduced in Eq. (2) and obtained by fitting the data plotted in Fig. 7.

p	a_2	b_2	p	a_2	b_2
0.001	0	0.000131	0.07	0	0.008424
0.003	0	0.000376	0.1	0	0.011714
0.005	0	0.000626	0.3	0	0.030739
0.007	0	0.000877	0.5	0	0.045562
0.01	0	0.001220	0.7	0	0.057753
0.03	0	0.003608	1.0	0	0.071680
0.05	0	0.006034			

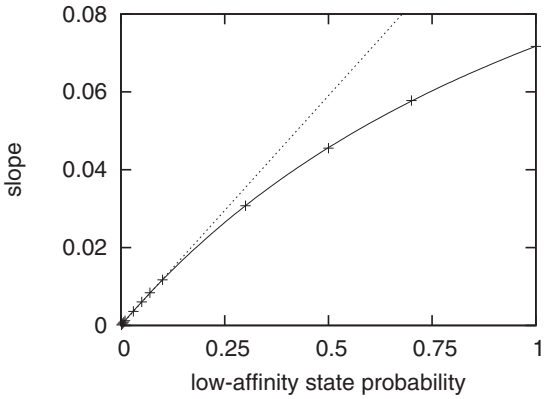

FIG. 8. Plot of the slope coefficient b_2 introduced in Eq. (2) as a function of the low-affinity state probability p. The dotted straight line has been obtained by fitting the data with the function $b_2 = a_3 + b_3 p$ on the interval [0,0.1]; the result of the fit is $a_3 = 0$ and $b_3 = 0.118$. The solid line has been obtained by fitting the data with the function $b_2 = p/(a'_3 + b'_3 p)$ on the whole data set, that is, on the interval [0,1]; the result of the fit is $a'_3 = 7.96$ and $b'_3 = 5.98$; note that the derivative in 0 is $1/a'_3 = 0.1256 \approx b_3$.

the time fraction spent by the pore in the low-affinity state is large, the potassium flux is, with good approximation, directly proportional to its density in the bulk. On the other hand, when the time fraction spent by the filter in the low-affinity state is smaller, the potassium flux exhibits a sublinear behavior with density.

Finally, in Fig. 11 the potassium flux as a function of the low-affinity state probability p is reported.

VI. ANALYTICAL STUDY

In this section we analytically study the basic model introduced in Sec. II in order to give a physical interpretation of the behavior of sodium and potassium flux on the species density and on the low-affinity state probability. In our model the pore is modeled in a very simple fashion, indeed it is just a two state Bernoulli process; the main difficulty is, obviously, the interaction between the random walk inside the volume Λ

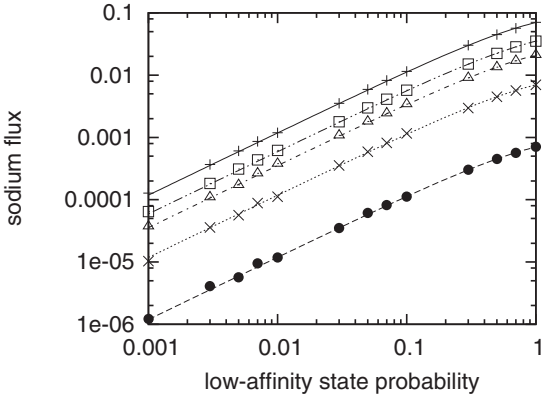

FIG. 9. Log-log plot of the sodium flux $\bar{f}_{\mathrm{Na}}$ as a function of the low-affinity state probability p. Data refers to the cases $N_{\mathrm{Na}} = 100(\bullet)$, $1000(\times)$, $3000(\triangle)$, $5000(\square)$, $10\,000(+)$. Lines are the graph of the function (3) with the appropriate values of ϱ_{Na}.

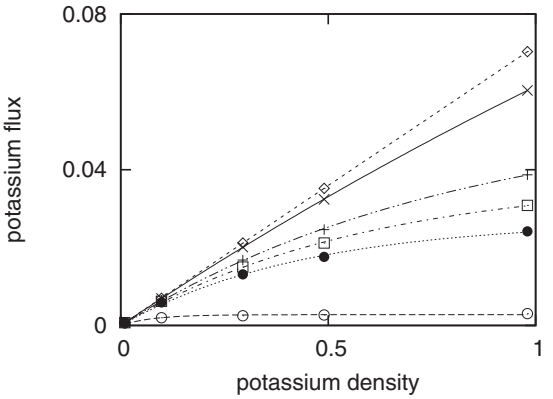

FIG. 10. Potassium flux $\bar{f}_{\mathrm{K}}$ as a function of the potassium density ϱ_{K}. Data in the picture refers to the cases $p = 0.005(\bigcirc)$, $0.05(\bullet)$, $0.07(\square)$, $0.1(+)$, $0.3(\times)$, $1.0(\diamond)$. The other values of p are not shown: the behavior is similar. Lines are drawn to guide the eyes.

and the pore itself. We consider the stationary state reached by a walker and denote by q_{K} (q_{Na}) the probability for a potassium (sodium) ion to occupy the site x of Λ neighboring the pore.

Since sodium particles can exit the system only when the pore is in the low-affinity state, the sodium flux is simply given by

$$f_{\mathrm{Na}} = \tfrac{1}{8} N_{\mathrm{Na}} q_{\mathrm{Na}} p, \tag{4}$$

where, we recall, N_{Na} is the number of sodium ions in the volume Λ. Indeed, the probability for a sodium ion to be on the site x neighboring the pore is q_{Na}, the probability for such a particle to jump to the pore itself is $1/4$ and, once in the pore, the probability to really exiting the system is $1/2$.

When dealing with potassium, one has to take into account that, when the pore switches to the low-affinity state, the possibly trapped potassium ion is released with probability one half. We then have for the potassium flux

$$f_{\mathrm{K}} = \tfrac{1}{8} N_{\mathrm{K}} q_{\mathrm{k}} p + \tfrac{1}{2} p r, \tag{5}$$

where we have denoted by r the stationary probability for the pore to be occupied by one of the N_{K} potassium particles.

The problem now is that of computing the stationary probabilities q_{Na},q_{K}, and r. The following study is related to

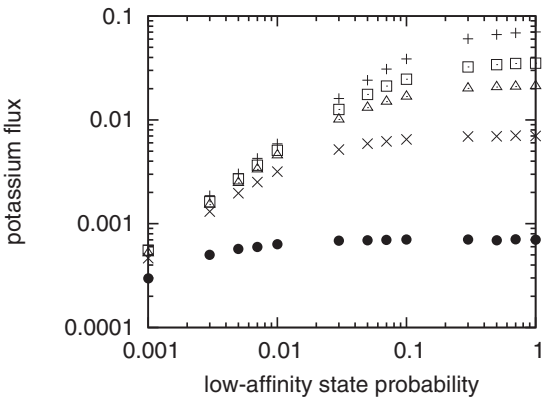

FIG. 11. Log-log plot of the potassium flux $\bar{f}_{\mathrm{K}}$ as a function of the low-affinity state probability p. Data refers to the cases $N_{\mathrm{K}} = 100(\bullet)$, $1000(\times)$, $3000(\triangle)$, $5000(\square)$, $10\,000(+)$.

the two-dimensional model discussed in the above sections; in Appendix B we address the same problem in the one-dimensional case, which is an interesting case, since some of the involved computations can be performed exactly. The related results will both support our two-dimensional approximate discussion and confirm the reliability of our Monte Carlo measurements.

We first consider the sodium case. An obvious guess is that the probability q_{Na} is $q_{\mathrm{Na}}^{(0)} = 1/|\Lambda|$, that is, it is uniform throughout the system. In this way we get

$$f_{\mathrm{Na}}^{(0)} = \frac{1}{8} N_{\mathrm{Na}} \frac{1}{L^2} p. \tag{6}$$

Note that this simple model provides the estimate 8 for the constant $a_3' = 7.96$, obtained by fitting the data in Fig. 8, and 0 for the constant $b_3' = 5.98$. The comparison between the Monte Carlo data and the theoretical prediction $f_{\mathrm{Na}}^{(0)}$ is good for small values of the low-affinity state probability, while (see Fig. 12) the experimental data departs from the predicted behavior for large p.

This behavior is not surprising: at large p the outgoing flux is so important that one has to expect a sort of depletion of the region close to the pore. To estimate this effect we develop a sort of "mean field" argument: we imagine that in all the sites of Λ different from the one neighboring the pore the stationary probability $q_{\mathrm{Na},0}$ is uniform. To get the stationary probability q_{Na} in the site x close to the pore we make the following probability balance:

$$q_{\mathrm{Na}} = \frac{3}{4} q_{\mathrm{Na},0} + \frac{1}{4}(1-p) q_{\mathrm{Na}} + \frac{1}{4}\frac{1}{2} p q_{\mathrm{Na}} + \frac{1}{4}\frac{1}{2L^2} p q_{\mathrm{Na}},$$

where, on the right-hand side, the first term is the probability that the particle moves from $\Lambda \setminus \{x\}$ to x, whereas the other terms take into account the probability that the particle in x remains in x. The above equation, together with the obvious normalization condition,

$$(L^2 - 1) q_{\mathrm{Na},0} + q_{\mathrm{Na}} = 1$$

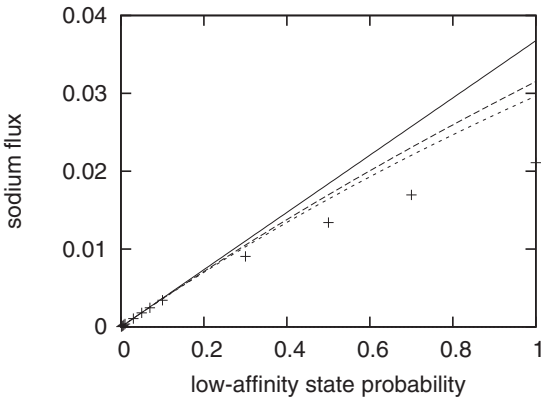

FIG. 12. Sodium flux as function of the low-affinity state probability. Pluses are the Monte Carlo results for $N_{\mathrm{Na}} = 3000$. The solid, long dashed, and short dashed lines are the corresponding graphs of the functions $f_{\mathrm{Na}}^{(0)}(p)$, $f_{\mathrm{Na}}^{(1)}(p)$, and $f_{\mathrm{Na}}^{(2)}(p)$, respectively.

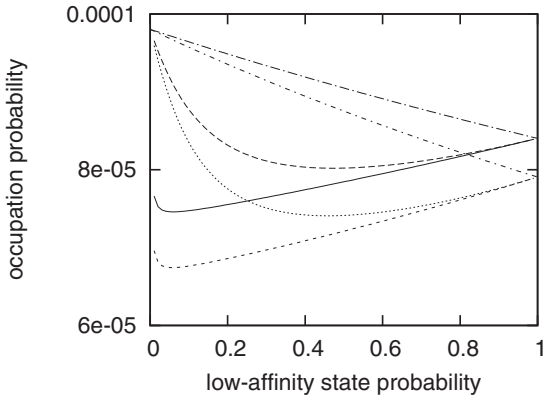

FIG. 13. Referring to the left side of the picture, from the top to the bottom the graphs of the functions $q_{\mathrm{Na}}^{(1)}(p)$, $q_{\mathrm{Na}}^{(2)}(p)$, $q_{\mathrm{K}}^{(1)}(p)$, and $q_{\mathrm{K}}^{(2)}(p)$ for $N_{\mathrm{K}} = 10\,000$, $q_{\mathrm{K}}^{(1)}(p)$ and $q_{\mathrm{K}}^{(2)}(p)$ for $N_{\mathrm{K}} = 100$, are plotted.

yields

$$q_{\mathrm{Na}}^{(1)} = \frac{1}{L^2 + p(L^2-1)^2/(6L^2)}$$

for the occupation probability and, hence,

$$f_{\mathrm{Na}}^{(1)} = \frac{1}{8} N_{\mathrm{Na}} \frac{p}{L^2 + p(L^2-1)^2/(6L^2)}$$

for the sodium outgoing flux. This approximation provides the estimate 8 for the constant $a_3' = 7.96$, obtained by fitting the data in Fig. 8, and $4(L^2-1)^2/(3L^4) = 1.33$ for the constant $b_3' = 5.98$. The graph of the occupation probability is plotted in Fig. 13; the guessed depletion effect is found and the occupation probability decreases when p is increased.

For small p and large L, $f_{\mathrm{Na}}^{(1)} \approx f_{\mathrm{Na}}^{(0)}$; this is reasonable, since in this limit the depletion effect is negligible. As it is shown in Fig. 12 the function $f_{\mathrm{Na}}^{(1)}$ is a quite good approximation of the experimental data, which, as we have seen above, are perfectly fitted by the function $\bar{f}_{\mathrm{Na}}$ given in Eq. (3).

A more detailed description of the dynamics close to the pore can yield a better estimate of the depletion effect. Consider one of the N_{Na} walkers on Λ and let, as we did before, q_{Na} be the probability that it occupies the site x in Λ, neighboring the pore. Say that the boundary is along the north-south direction and that the pore is to the east of the site x. Let $q_{\mathrm{Na},1}$ be the probability that the particle is on the site to the north of x and that it is equal to the probability that the walker occupies the site to the south. Let $q_{\mathrm{Na},2}$ be the probability that the particle is on the site to the west of x. Assume that for the remaining $L^2 - 4$ sites of the lattice the occupation probability is $q_{\mathrm{Na},0}$.

As before it is not difficult to write the following probability balance equations:

$$\begin{aligned} q_{\mathrm{Na},1} &= 2q_{\mathrm{Na},0}/4 + q_{\mathrm{Na}}/4 + q_{\mathrm{Na},1}/4, \\ q_{\mathrm{Na},2} &= 3q_{\mathrm{Na},0}/4 + q_{\mathrm{Na}}/4, \\ q_{\mathrm{Na}} &= q_{\mathrm{Na},2}/4 + 2q_{\mathrm{Na},1}/4 + (1-p) q_{\mathrm{Na}}/4 + p q_{\mathrm{Na}}/8, \end{aligned}$$

where we have neglected the terms proportional to $1/L^2$. The above equations, together with the obvious normalization

condition

$$(L^2-4)q_{\mathrm{Na},0}+q_{\mathrm{Na},2}+2q_{\mathrm{Na},1}+q_{\mathrm{Na}}=1$$

yield

$$q_{\mathrm{Na}}^{(2)}=\frac{12/23}{1+12(1+6p/25)(L^2-23/12)/23}$$

for the occupation probability and, hence,

$$f_{\mathrm{Na}}^{(2)}=\frac{1}{8}N_{\mathrm{Na}}\frac{1}{L^2+6p(L^2-23/12)/25}p$$

for the sodium outgoing flux. This approximation provides the estimate 8 for the constant $a_3'=7.96$, obtained by fitting the data in Fig. 8, and $48(1-23/(12L^2))/25=1.92$ for the constant $b_3'=5.98$. Note that for small p and large L, $f_{\mathrm{Na}}^{(2)}\approx f_{\mathrm{Na}}^{(0)}$. As it is shown in Fig. 12 the function $f_{\mathrm{Na}}^{(2)}$ is a better approximation of the experimental data with respect to $f_{\mathrm{Na}}^{(1)}$ and $f_{\mathrm{Na}}^{(0)}$.

The graph of the occupation probability $q_{\mathrm{Na}}^{(2)}(p)$ is plotted in Fig. 13; the depletion effect is more pronounced with respect to that described by the approximation $q_{\mathrm{Na}}^{(1)}(p)$.

We now come to the computation of the potassium flux. We consider a potassium walker and we note that for such a particle the random walk is performed in $\Lambda\cup\{\text{pore}\}$. We assume that in the stationary state the probability that the potassium walker is in the pore is r/N_{K}. Thus in the stationary state

$$\frac{r}{N_{\mathrm{K}}}=\frac{1}{4}(1-p)(1-r)q_{\mathrm{K}}+(1-p)\frac{r}{N_{\mathrm{K}}},$$

where, we recall, q_{K} is the probability that the potassium ion occupies the site x in Λ neighboring the pore. Indeed, by stationarity, the probability that the particle is in the pore is equal to the probability that the pore is empty in the high-affinity state and that the particle jumps from x to it plus the probability that the pore is occupied and in the high-affinity state. From the equation above we easily get

$$r=\frac{1}{4}N_{\mathrm{K}}q_{\mathrm{K}}(1-p)\frac{1}{p+N_{\mathrm{K}}q_{\mathrm{K}}(1-p)/4}. \tag{7}$$

Then we have to estimate q_{K}. As we have done in the case of sodium we first consider the stationary occupation probability uniform inside the volume Λ and equal to $q_{\mathrm{K}}^{(0)}=1/L^2$. The corresponding probability $r^{(0)}$ for the pore to be occupied is given by Eq. (7) and the corresponding potassium flux $f_{\mathrm{K}}^{(0)}$, given by (5), is plotted in Fig. 14. The comparison with the experimental data is very good at small low-affinity probability p, while the experimental results depart from the predicted behavior at large p.

As before this is due to the depletion of the region close to the pore. We repeat the same computation described in detail for the sodium particles. Here we just give the main formulas: the first approximation consists in the probability

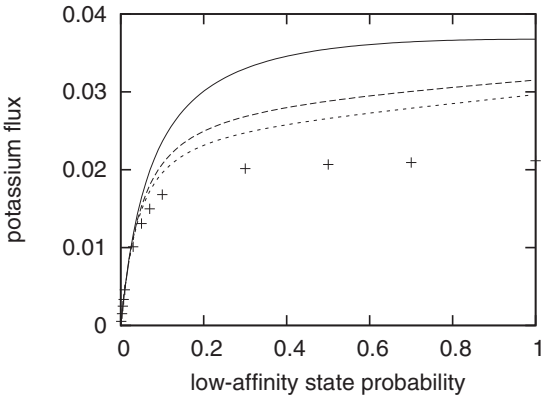

FIG. 14. Potassium flux as function of the low-affinity state probability. Pluses are the Monte Carlo results for $N_{\mathrm{K}}=3000$. The solid, broken (large), broken (small), dotted lines are the corresponding graphs of the functions $f_{\mathrm{K}}^{(0)}(p)$, $f_{\mathrm{K}}^{(1)}(p)$, and $f_{\mathrm{K}}^{(2)}(p)$, respectively.

balance equation

$$q_{\mathrm{K}}=\frac{3}{4}q_{\mathrm{K},0}+\frac{1}{8}q_{\mathrm{K}}p+\frac{1}{8L^2}q_{\mathrm{K}}p+\frac{1}{4}q_{\mathrm{K}}(1-p)r+\frac{1}{2L^2}p\frac{r}{N_{\mathrm{K}}}+\frac{1}{2}p\frac{r}{N_{\mathrm{K}}}$$

By using the obvious normalization condition $(L^2-1)q_{\mathrm{K},0}+q_{\mathrm{K}}+r/N_{\mathrm{K}}=1$, by neglecting all the terms proportional to $1/L^2$ and to $1/N_{\mathrm{K}}$, and by recalling Eq. (7), we get

$$r^{(1)}=\frac{AD+Bp-\sqrt{(AD+Bp)^2-4ACDp}}{2Cp}$$

and

$$q_{\mathrm{K}}^{(1)}=\frac{A}{B-Cr^{(1)}},$$

where

$$A=\frac{3}{4}\frac{1}{L^2-1},\quad B=A+1-\frac{1}{8}p,\quad C=\frac{1}{4}(1-p),$$

and

$$D=CN_{\mathrm{K}}.$$

The corresponding potassium flux $f_{\mathrm{K}}^{(1)}$ given by (5) is depicted in Fig. 14. The improvement with respect to $f_{\mathrm{K}}^{(0)}$ is striking.

We can further improve the way in which the depletion effect is estimated as we did for the sodium particles. By neglecting, as we did above, contributions proportional to $1/L^2$ and to $1/N_{\mathrm{K}}$, we get the probability balance equations

$$\begin{aligned}2q_{\mathrm{K},0}/4+q_{\mathrm{K}}/4-3q_{\mathrm{K},1}/4=0,\\ 3q_{\mathrm{K},0}/4-q_{\mathrm{K},2}+q_{\mathrm{K}}/4=0,\\ q_{\mathrm{K},2}/4+2q_{\mathrm{K},1}/4-3q_{\mathrm{K}}/4-q_{\mathrm{K}}p/8\\ -(1-p)q_{\mathrm{K}}(1-r)/4=0,\end{aligned}$$

and the obvious normalization condition

$$(L^2-4)q_{\mathrm{K},0}+q_{\mathrm{K},2}+2q_{\mathrm{K},1}+q_{\mathrm{K}}=1.$$

The above equations, together with (7), yields for $r^{(2)}$ and $q_K^{(2)}$ the same expression as those for $r^{(1)}$ and $q_K^{(1)}$ with

$$A = \frac{25}{48}\frac{1}{L^2 - 23/12} \quad \text{and} \quad B = \frac{23}{12}A + \frac{37}{48} - \frac{1}{8}p,$$

whereas C and D are as before. The corresponding potassium flux $f_K^{(2)}$, given by (5) and plotted in Fig. 14, improves the estimate $f_K^{(1)}$.

We finally comment on the behavior of the occupation probability q_K as function of the low-affinity state probability p. In Fig. 13 we have plotted $q_K^{(1)}$ and $q_K^{(2)}$ for $N_K = 100$ and $N_K = 10\,000$. We note that those curves tend to the same value of the corresponding curves for the sodium occupation probability when p tends to one. This proves that the approximations are coherent, indeed, in this limit sodium and potassium particles behave similarly. We also note that sodium occupation probabilities are decreasing functions of the low-affinity state probability p. For potassium ions the occupation probability decreases at small p and increases at large p. This is due to the fact that at large p the probability r that the pore is occupied is small and so is the associated contribution to the potassium flux.

VII. CONCLUSIONS

Potassium channels are special transmembrane proteins allowing selected potassium permeation outside cells. Gating and selectivity attitudes are not fully understood. For special K^+-channel types it has been supposed that gating is realized via a selectivity filter. In this paper we have proposed and studied a lattice model, in the same spirit of [18], in which a pore selection rule ensures both selection and gating. This model has been studied both by means of a Monte Carlo method and via an analytical approximation. We have estimated both potassium and sodium fluxes through the membrane.

We have proven the possibility of achieving selection and gating and we have discussed the potassium flux reduction due to the presence of the selectivity filter. In particular we have shown that allowing more than one potassium ion at time to be accommodated inside the pore the potassium flux loss is completely recovered when physiological cytosolic densities are considered. We then conclude that gating can be achieved via a selectivity filter in an efficient way.

We have also studied extensively the model discussing the behavior of potassium and sodium fluxes as functions of the interesting physiological parameters, that is, the ionic cytosolic density and the time fraction the filter spends in the low-affinity state. It is remarkable to notice that the flux of the ionic species which is not affected by the selectivity filter, sodium in our model, is directly proportional to the cytosolic density. A sublinear behavior is found for potassium

In conclusion, we think that lattice models provide essential and tunable tools to investigate efficiently the properties of ionic channels by analyzing the wealth of experimental data available on this subject.

ACKNOWLEDGMENTS

All numerical simulations have been performed on two SUN FIRE 2100 servers of the Dipartimento di Scienze di Base e Applicate per l'Ingegneria (SBAI). We express our thanks to an anonymous referee for very useful comments.

APPENDIX A: DETAILED DEFINITION OF THE MODEL

In this section we describe in detail the Monte Carlo scheme that we have studied and whose behavior has been discussed above.

We consider an integer *time* variable t. We set $t = 0$ and choose at random with uniform probability $1/L^2$ the position of the N_{Na} sodium particles and the N_K potassium particles. We then repeat the following *steps* until t equals the given integer number t_{max}:

(1) Set t equal $t + 1$.

(2) Select at random the state of the pore: choose the low-affinity state with probability p and the high-affinity one with probability $1 - p$.

(2a) If the pore is in the low-affinity state and it is occupied by a particle, the particle is released with the following rule: it jumps with probability $1/2$ to the site of Λ neighboring the pore or (with the same probability) it exits the system.

(2b) If a particle exits the system, a particle of the same species is put at random with uniform probability $1/L^2$ on one of the L^2 sites in Λ.

(3) The position of each particle on the lattice is updated following the rules defined in Fig. 1.

(3a) If a particle enters the pore and the pore is in the low-affinity state, the particle is immediately released by the pore with the following rule: it jumps with probability $1/2$ to the site of Λ neighboring the pore or (with the same probability) it exits the system.

(3b) If a particle exits the system, a particle of the same species is put at random with uniform probability $1/L^2$ on one of the L^2 sites in Λ.

We considered a second model with the aim of improving the potassium flux efficiency at low-affinity state probability. This model is defined as the basic one with a single difference: the rule for a potassium ion in the site neighboring the pore when the pore is occupied and in the high-affinity state (see the right top part of Fig. 1) is the same experienced when the pore is free in the high-affinity state.

APPENDIX B: ONE-DIMENSIONAL MODEL

The basic model introduced in Sec. II can be easily specialized to the one-dimensional case. The lattice is $\Lambda = \{1, \ldots, L\}$ and the pore is the site $L + 1$ of $\mathbb{Z}$. Equations (4) and (5) become

$$f_{Na} = \tfrac{1}{4} N_{Na} q_{Na} p \tag{B1}$$

and

$$f_K = \tfrac{1}{4} N_K q_k p + \tfrac{1}{2} p r. \tag{B2}$$

In order to compute q_{Na} we consider the random walk of a single sodium ion on the lattice $\{1,\ldots,L\}$. The transition matrix elements different from zero are

$$\pi_{i,i+1} = \tfrac{1}{2} \quad \text{for} \quad i = 1,\ldots,L-1$$

for nearest-neighbor jumps to the right,

$$\pi_{i+1,i} = \tfrac{1}{2} \quad \text{for} \quad i = 1,\ldots,L-2$$

for nearest-neighbor jumps to the left,

$$\pi_{L,L-1} = \tfrac{1}{2} + \tfrac{1}{4L}p$$

for the nearest-neighbor jump to the left starting from the site L,

$$\pi_{L,i} = \frac{1}{4L}p \quad \text{for} \quad i = 1,\ldots,L-2$$

for left jumps starting from the site L (this not zero transition matrix elements are due to the fact that particles exiting the system are put at random with uniform probability in one site of the lattice Λ), and finally

$$\pi_{1,1} = \frac{1}{2} \quad \text{and} \quad \pi_{L,L} = \frac{1}{4}p + \frac{1}{4L}p + \frac{1}{2}(1-p).$$

We let q_i, with $i = 1,\ldots,L$, be the stationary probability that the walker occupies the site i. Since the pore is the site $L+1$ of $\mathbb{Z}$, we have that q_{Na} is nothing but q_L. Recalling the definition of stationary measure

$$q_i = \sum_{j=1}^{L} \pi_{i,j} q_j$$

for $i = 1,\ldots,L$, we have

$$\begin{aligned}
q_1 &= \frac{1}{2}q_1 + \frac{1}{2}q_2 + \frac{1}{4L}pq_L,\\
q_2 &= \frac{1}{2}q_1 + \frac{1}{2}q_3 + \frac{1}{4L}pq_L,\\
&\vdots\\
q_{L-1} &= \frac{1}{2}q_{L-2} + \frac{1}{2}q_L + \frac{1}{4L}pq_L,\\
q_L &= \frac{1}{2}q_{L-1} + \frac{1}{4}pq_L + \frac{1}{4L}pq_L + \frac{1}{2}(1-p)q_L.
\end{aligned} \tag{B3}$$

By using the first $L-1$ Eqs. (B3) by recursion we get

$$q_k = q_{k+1} + \frac{k}{2L}pq_L \tag{B4}$$

for $k = 1,\ldots,L-1$. By recursion, again, it is also easy to prove that (B4) implies

$$q_{L-i} = q_L + \frac{2iL - i(i+1)}{4L}pq_L \tag{B5}$$

for $i = 1,\ldots,L-1$, so that the probabilities $q_1,\ldots,q_{L-1}$ are all expressed in terms of q_L. Note that q_{L-i} decreases when i runs from $L-1$ to 1, so that the depletion phenomenon discussed in Sec. VI is found also in the one-dimensional case.

In order to find q_L, we finally require that the normalization condition

$$q_1 + \cdots + q_L = 1$$

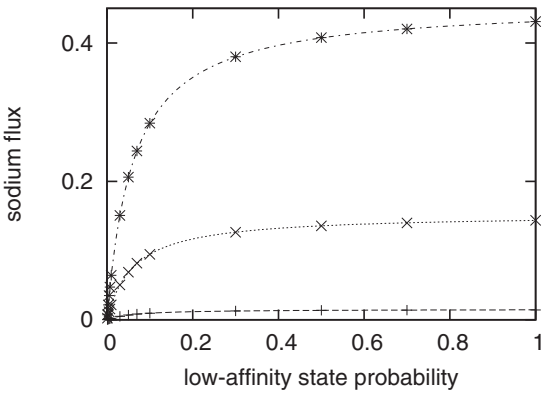

FIG. 15. Sodium flux as function of the low-affinity state probability in the one-dimensional case for $L = 100$. The points $*$, $\times$, and $+$ are the Monte Carlo results, respectively, for $N_{\mathrm{Na}} = 3000$, 1000, 100. The three lines are the graphs of the function (B1) with q_{Na} given by (B6) for the corresponding values of N_{Na}.

is satisfied. A straightforward computation yields

$$q_L = \frac{1}{L + (2L^2 - 3L + 1)p/12}. \tag{B6}$$

The one-dimensional sodium flux can be finally computed by using (B1) with q_{Na} given by (B6). Monte Carlo results are compared with this theoretical prediction in Fig. 15 and the matching is perfect.

The computation of q_{K} is more difficult, since the interaction between the potassium ions and the pore is not as trivial as for sodium. In particular, due to the possibility that a potassium ion is trapped in the pore, the potassium walkers cannot be considered independent. We shall treat this case by assuming that in the stationary state the probability for the pore to be occupied by one of the N_{K} potassium ions is r. We then study a potassium walker on the lattice $\Lambda = \{1,\ldots,L,L+1\}$, where the site $L+1$ is the pore, and at the end we shall require that $q_{L+1} = r/N_{\mathrm{K}}$. In other words, we shall finally assume that, in the stationary state, the probability for a single walker to occupy the pore is equal to the probability that the pore is occupied by one of the walkers divided by the number of potassium ions.

We do not list all the not zero transition matrix elements, but only those differing from the sodium case:

$$\pi_{L+1,i} = \frac{1}{2L}p \quad \text{for} \quad i = 1,\ldots,L-1$$

due to particles released by the pore when it flips to the low-affinity state, and

$$\begin{aligned}
\pi_{L,L} &= p/4 + p/(4L) + (1-p)r/2,\\
\pi_{L,L+1} &= (1-p)(1-r)/2,\\
\pi_{L+1,L} &= p/2 + p/(2L),\\
\pi_{L+1,L+1} &= (1-p)
\end{aligned}$$

for the interaction between the pore and its neighboring site.

Now we repeat the same computation as in the sodium case. We first exploit the definition of the stationary measure to

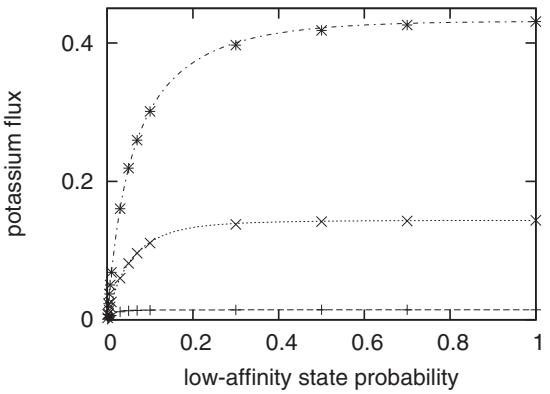

FIG. 16. Potassium flux as function of the low-affinity state probability in the one-dimensional case for $L = 100$. The points $*$, $\times$, and $+$ are the Monte Carlo results respectively for $N_K = 3000, 1000, 100$. The three lines are the graphs of the function (B2) with q_K given by (B10) and r given by (B9) for the corresponding values of N_K.

write

$$\begin{aligned}
q_1 &= \frac{1}{2}q_1 + \frac{1}{2}q_2 + \frac{1}{4L}pq_L + \frac{1}{2L}pq_{L+1},\\
q_2 &= \frac{1}{2}q_1 + \frac{1}{2}q_3 + \frac{1}{4L}pq_L + \frac{1}{2L}pq_{L+1},\\
&\vdots\\
q_{L-1} &= \frac{1}{2}q_{L-2} + \frac{1}{2}q_L + \frac{1}{4L}pq_L + \frac{1}{2L}pq_{L+1},\\
q_L &= \frac{1}{2}q_{L-1} + \frac{1}{4}pq_L + \frac{1}{4L}pq_L + \frac{1}{2}(1-p)rq_L\\
&\quad + \frac{1}{2}pq_{L+1} + \frac{1}{2L}pq_{L+1},\\
q_{L+1} &= \frac{1}{2}(1-p)(1-r)q_L + (1-p)q_{L+1}.
\end{aligned} \tag{B7}$$

As for the sodium we obtain

$$q_{L-i} = q_L + \frac{2iL - i(i+1)}{4L}pq_L + \frac{2iL - i(i+1)}{2L}pq_{L+1} \tag{B8}$$

for $i = 1, \ldots, L-1$, so that the probabilities $q_1, \ldots, q_{L-1}$ are all expressed in terms of q_L and q_{L+1}. By combining (B8) with the expression of q_L in (B7) we get

$$q_L = \frac{2p}{(1-p)(1-r)}q_{L+1},$$

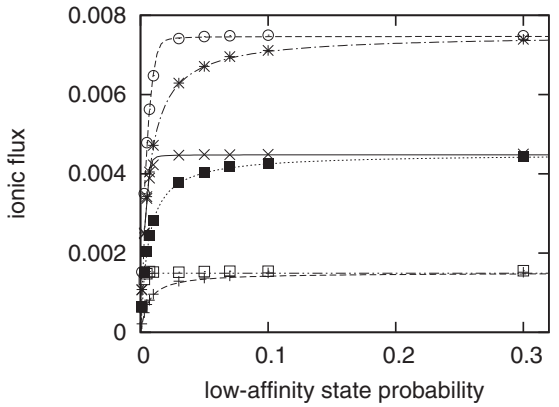

FIG. 17. Sodium and potassium flux as function of the low-affinity state probability in the one-dimensional case for $L = 1000$. The points $+$, $\blacksquare$, and $*$ are the Monte Carlo estimates of the sodium flux, respectively, for $N_{Na} = 1000, 3000, 5000$. The points $\square$, $\times$, and $\circ$ are the Monte Carlo estimates of the potassium flux respectively for $N_K = 1000, 3000, 5000$. The lines are the graphs of the function (B1) and (B2) for the corresponding values of N_{Na} and N_K.

which is obviously equivalent to the last equation in (B7).

As discussed above, we finally assume $q_{L+1} = r/N_K$ and, by exploiting the normalization condition $q_1 + \cdots + q_L + q_{L+1} = 1$, we get

$$r = \frac{N_K + B + C - \sqrt{(N_K + B + C)^2 - 4N_K C}}{2C} \tag{B9}$$

and

$$q_L = \frac{2p}{(1-p)(1-r)}\frac{r}{N_K}, \tag{B10}$$

where we have set

$$A = \frac{2L^2 - 3L + 1}{3}, \quad B = \frac{2p}{1-p}\left(L + \frac{1}{4}Ap\right),$$
$$C = 1 + \frac{1}{2}pA.$$

The one-dimensional potassium flux can be finally computed by using (B2) with q_K given by (B10). Monte Carlo results are compared with this theoretical prediction of r in Fig. 16 and the matching is perfect.

In Fig. 17 we have compared Monte Carlo and analytical results for $L = 1000$. Graphs have been plotted on the same figures in order to show that even in the one-dimensional case the selection effect can be appreciated.

[1] A. L. Hodgkin and A. F. Huxley, J. Physiol. **116**, 473 (1952).
[2] E. Neher and B. Sakmann, Nature (London) **260**, 799 (1976).
[3] B. Hille, *Ion Channels of Excitable Membranes*, 3rd ed. (Sinauer Associates, Sunderland, MA, 2001).
[4] S. A. N. Goldstein, D. Bockenhauer, I. O'Kelly, and N. Zilberberg, Nat. Rev. Neurosci. **2**, 175 (2001).
[5] A. M. J. VanDongen, Comm. Theor. Biol. **2**, 429 (1992).
[6] C. Miller, Genome Biol. **1**, reviews0004 (2000).
[7] D. Fedida and J. C. Hesketh, Prog. Bio. Mol. Biology **75**, 165 (2001).
[8] M. Recanatini, A. Cavalli, and M. Masetti, Chem. Med. Chem. **3**, 523 (2008).
[9] B. Sakmann and E. Neher, Ann. Rev. Physiol. **46**, 455 (1984).
[10] A. Abenavoli, M. L. Di Francesco, I. Schroeder, S. Epimoshko, S. Gazzarini, U. P. Hansen, G. Thiel, and A. Moroni, J. Gen. Physiol. **134**, 219 (2009).

[11] Y. Zhou and R. Mackinnon, J. Mol. Biol. **333**, 965 (2003).
[12] J. Åqvist and V. Luzhkov, Nature (London) **404**, 881 (2000).
[13] C. Miller, J. Gen. Physiol. **113**, 783 (1999).
[14] P. H. Nelson, J. Chem. Phys. **117**, 11396 (2002).
[15] P. H. Nelson, Phys. Rev. E **68**, 061908 (2003).
[16] P. H. Nelson, J. Chem. Phys. **134**, 165102 (2011).
[17] S. Mafé and J. Pellicer, Phys. Rev. E **71**, 022901 (2005).
[18] A. M. J. VanDongen, PNAS **101**, 3248 (2004).
[19] S. Choe, Nat. Rev. Neurosci. **3**, 115 (2002).
[20] K. J. Swartz, Nat. Rev. Neurosci. **5**, 905 (2004).
[21] D. Andreucci and D. Bellaveglia, preprint Dipartimento SBAI 3 (2011), [www.dmmm.uniroma1.it/preprints.it.php?tipopubb=p] (to appear).